Published in final edited form as:
Muscle Nerve. 2010 December ; 42(6): 901–907. doi:10.1002/mus.21788.

Nemaline myopathy type 6: clinical and myopathological features

Montse Olivé, MD[a], **Lev G Goldfarb, MD**[b], **Hee-Suk Lee, MD**[b], **Zagaa Odgerel, PhD**[b], **Andre Blokhin, MD**[c], **Laura Gonzalez-Mera, MD**[a], **Dolores Moreno, Tch**[a], **Nigel G Laing, PhD**[d], and **Nyamkhishig Sambuughin, PhD**[c]

[a] Institute of Neuropathology, Pathology Department, IDIBELL-Hospital de Bellvitge and CIBERNED, Hospitalet de Llobregat, Barcelona, Spain

[b] National Institute of Neurological Disorders and Stroke, National Institutes of Health, Bethesda, Maryland, U.S.A

[c] Uniformed Services University of the Health Sciences, Bethesda, Maryland, U.S.A

[d] University of Western Australia, Center for Medical Research, Western Australian Institute for Medical Research, QEII Medical Centre, Western Australia, Australia

Abstract

Introduction—Nemaline myopathy (NEM) is one of the most common congenital myopathies. A unique subtype, NEM6, maps to chromosome 15q21-q23 in two pedigrees, but the causative gene has not been determined.

Methods—We conducted clinical examination and myopathological studies in a new NEM family. Genotyping and gene screening were accomplished by searching known and 18 new candidate genes.

Results—The disease started in childhood by affecting proximal and distal muscles and causing slowness of movements. Muscle biopsies show numerous nemaline rods and core-like formations. Suggestive linkage to chromosome 15q22-q23 was established. Genes known to be mutated in NEM or core-rod myopathy were screened and excluded. No pathogenic mutations were identified in other candidate genes.

Discussion—The disease in this Spanish family is classified as NEM6. It is phenotypically similar and probably allelic to the two previously reported NEM6 pedigrees. Further studies of these families will lead to the identification of the NEM6 gene.

Keywords

Nemaline myopathy; core-rod myopathy; NEM6; Spanish family; chromosome 15q

Introduction

Nemaline myopathy (NEM) is a congenital myopathy that is characterized clinically by proximal muscle weakness and hypotonia and defined morphologically by eosinophilic rod-shaped inclusions or nemaline bodies in muscle fibers [1–4]. Several clinical types of NEM are recognized based on the age of disease onset and severity of muscle weakness, ranging

Correspondence: Montse Olivé, Institut de Neuropatologia, IDIBELL-Hospital de Bellvitge and CIBERNED, Feixa Llarga s/n, Hospitalet de Llobregat, 08907 Barcelona, Spain, Tel./fax: +34 93 260 7503, 25169mop@comb.cat.

from a severe neonatal often lethal subtype to milder non-progressive or slowly progressive forms that present in infancy, childhood or adulthood [5–7]. Muscle weakness may be diffuse, but it is often most pronounced in the face, neck and proximal limb muscles. Pharyngeal and respiratory muscles are frequently affected [5]. Distal weakness appears late in the course of illness, but in some forms manifests at presentation [8]. The pattern of inheritance is also variable; autosomal recessive, autosomal dominant, and sporadic cases have been reported [8–11]. Nemaline bodies are rod-shaped structures continuous with and derived from the Z-disks [12]. α-actinin is the major component of a nemaline rod [13,14]. Other Z-disc proteins including myotilin and nebulin are also expressed in rods [15,16]. Type I fiber predominance and atrophy or hypertrophy are other common features of nemaline myopathy [5,12,17].

Mutations that cause nemaline myopathy have been identified in *α*-actin (*ACTA1*), *α*-and *β*-tropomyosin (*TPM3* and *TPM2*), troponin T (*TNNT1*), nebulin (*NEB*), and cofilin2 (*CFL2*) [18]. Mutations in the ryanodine receptor (*RYR1*) [19,20] and nebulin (*NEB*) 21 have in some cases been found to be responsible for congenital core-rod myopathy. Recently, autosomal dominant nemaline myopathy in two families, Dutch 22 and Australian-Dutch 23, was mapped to a locus on chromosome 15q21-q23 with a combined LOD score of 10.65 at marker D15S993 [23] and named NEM6 (MIM 609273). Affected individuals in both reported families developed the disease in their infancy or childhood and experienced very slowly progressing weakness in the neck and proximal limb muscles with no facial, respiratory or distal muscle involvement. Each patient of the Dutch family manifested slowness of movements. Analysis of muscle biopsies in both families showed numerous rods and core-like structures [22,23].

We describe clinical, myopathological and genetic findings in a Spanish family with four cases fully consistent with published diagnostic criteria for nemaline myopathy [5,7]. The disease in this family maps to the 15q22.31 chromosomal locus fully congruent with the region previously identified in the larger Dutch and Australian-Dutch families.

MATERIALS AND METHODS

The Spanish family

Four patients with myopathy have been identified in a family that originated from Andalucia in Southern Spain (Figure 1). All affected and 7 unaffected family members underwent a clinical study that included general neurologic exam, muscle strength assessment according to the Medical Research Council (MRC) grading scale, serum CK test, and, if affected, nerve conduction testing and concentric needle EMG. Respiratory function tests and cardiological examination including ECG, 24-hour-Holter monitoring, and echocardiography were performed in individuals II:3 and II:5.

Muscle imaging

Muscle imaging studies were carried out in individuals II:3, II:5 and III:5 at the age of 60, 55 and 34 years, respectively. In patient II:3, transverse and coronal T1-weighted spin-echo (SE) and short-time inversion recovery (STIR) magnetic resonance imaging were performed on 1.5-T MR (Intera Philips, Amsterdam, The Netherlands). In patients II:5 and III:5, muscle imaging was performed using a helical CT scanner (HiSpeed NX/wiPRO, GE Medical Systems, Milwaukee, WI).

Myopathological Studies

Two patients (II:3 and II:5) underwent muscle biopsy at the age of 49 and 50 years. No muscle biopsies were performed during childhood. Samples obtained from the biceps brachii muscle were frozen in liquid nitrogen-cooled isopentane and processed for routine

histochemical reactions. Samples from patient II:5 were additionally processed for double labeling of myosin isoforms and desmin immunohistochemistry using antibodies against slow, fast, and developmental myosin (Novocastra, Newcastle upon Tyne, UK) at dilutions 1:100, 1:250, and 1:500, respectively, and desmin (Dako, Barcelona, Spain) at dilution 1:20. Immunofluorescence analysis was carried out by using antibodies against α-actinin (SIGMA, Saint Louis, Missouri, USA), myotilin (Novocastra, Newcastle upon Tyne, UK), and filamin C (mouse monoclonal anti-filamin C antibody RR90 kindly provided by DO Fürst) at dilutions 1:800, 1:200 and 1:25, respectively. The secondary antibody was Alexa 488 anti-mouse (Molecular Probes, Leyden, The Netherlands) used at dilution 1:400. Sections were mounted with Fluorescent Mounting Medium (DakoCytomation, Glostrup, Denmark), sealed and dried overnight at 4oC. A small piece of the muscle sample was processed for ultrastructural examination using standard methods.

Screening for Known Nemaline Myopathy Genes

Genomic DNA of patients II:3 and II:5 was tested for the presence of mutations in the coding regions of genes known or suspected to cause autosomal dominant nemaline myopathy: *ACTA1*, *TPM3*, *TPM2*, *TNNT1*, and *CFL2*. PCR amplification with intronic primers constructed to amplify each exon was carried out, and the resulting DNA fragments were sequenced using BigDyeTerminator™ protocol on an automated 3100 ABI Prism Genetic Analyzer (Applied Biosystems, Foster City, CA).

Genotyping

Genotyping of 11 members of the myopathy family was conducted with the use of markers from 15q21-q23, the previously identified NEM6 chromosomal interval, and 19q12-q13.2, the location of the candidate *RYR1* gene. Haplotypes were determined using marker allele segregation in the pedigree. LOD score for linkage was estimated by using the Fastlink package.

Search for causative Genes in the Candidate Chromosomal Region

Genomic DNA of patients II:3 and II:5 was also tested for mutations in the following genes positioned within the 15q21-q23 candidate region: *ANXA, TPM1, Talin2, LACT, RABB, HERC1, DAPK2, UPB3, PARP16, PPIB, MEMT, RASL12, CLPX, C15orf44, NOPE, SCL24A1, RAB11A, and DIS3L*. Techniques for PCR amplification and sequencing were the same as described above. Validation of genomic DNA sequencing results was accomplished by sequence analysis of complimentary DNA (cDNA) of *ACTA1*, *TPM3*, *TPM2*, *TNNT1*, *CFL2*, *TPM1*, *Talin2*, and *HERC1* transcripts, because they were considered supreme candidates to be involved in this disease. Total RNA was extracted from skeletal muscle biopsy tissue of patients II:3 and II:5 using the RNeasy Fibrous Tissue kit (Qiagen, Valencia, CA). One microgram of total RNA was used for reverse transcription reaction with MuLV Reverse Transcriptase (Applied Biosystems, Foster City, CA). Candidate mutations were detected by aligning with appropriate database entries (http://www.ncbi.nlm.nih.gov). The oligonucleotide sequences used for amplification are available on request.

RESULTS

Clinical Manifestations

Patients had a normal neonatal period and achieved normal motor milestones. They presented around 4 or 5 years of age with muscle weakness in the arms and legs manifested by gait abnormality and difficulties performing sports; they were unable to run or jump but could walk long distances. Each patient complained of difficulties opening a jar and lifting

heavy objects. The condition was very slowly progressive, with some acceleration in adulthood. On examination, all studied patients had proximal and distal muscle weakness in the upper and lower limbs. The deltoid and biceps muscles were weaker than the triceps (MRC score 4/5); forearm flexors and extensors and hand muscles were equally affected (MRC score 4/5). In the lower extremities, weakness was greatest in iliopsoas, hip adductors, anterior tibialis, and the peroneal group. The quadriceps muscle was strong in all affected individuals until late in the course of illness. Patients were unable to walk on heels but could stand on their toes. None had facial weakness. In only two members (II:1 and III: 5, Figure 1), neck flexors and paraspinal muscles were also affected. Muscle hypotrophy was present in the upper limbs, particularly in the forearm muscles (Figure 2). Slowness of movements that transformed into bradykinetic slow-motion behavior and clumsiness was a characteristic feature in each patient; patients were unable to sprint, had delayed startle reflexes, and were unable to correct their position to avoid falls. Deep tendon reflexes were preserved, except at the ankle; each patient had mild heel cord contracture. No cardiac or respiratory symptoms were present, and no clinical or electrophysiological evidence of peripheral neuropathy was detected. Three of 4 patients remained ambulant in their 30s to 60s. The oldest affected individual (II:2), now aged 74 years, is only able to walk short distances with support. CK levels were normal, and EMGs showed a myopathic pattern. Respiratory function tests and cardiological examination revealed no abnormalities.

Muscle MRI performed at the age of 60 years in individual II:3 showed diffuse involvement of thigh muscles, slightly more pronounced in the adductor magnus. At mid leg level there was a predominant involvement of the lateral and medial gastrocnemius, peroneal group and soleus, with less prominent changes in the anterior tibialis muscle. An identical pattern of muscle involvement was observed on a CT scan of his younger brother (II:5), but only minimal abnormalities were seen in a younger patient III:5 (Figure 3).

Myopathology

Muscle biopsy of case II:3 revealed marked variation in fiber size and increased number of internal nuclei (Figure 4A and B). There was mild endomysial fibrosis. A high proportion of fibers contained aggregates of abnormal fine, granular, or rod-shaped structures in the cytoplasm or in subsarcolemmal areas (Figure 4A and B); they were eosinophilic on HE stain (Figure 4B and C) and dark blue to red-purple on the modified trichrome stain (Figure 4A). There were a few ragged red fibers, and occasional fibers contained rimmed vacuoles (Figure 4C). In addition, some fibers harbored hyaline eosinophilic material beneath the sarcolemma or centrally within the cytoplasm (Figure 4B). In the muscle biopsy of patient II:5, typical nemaline rods were found in 90% of fibers (Figure 4D). They assembled into clusters in the subsarcolemmal areas (Figure 4E) or as masses within the cytoplasm (Figure 4F and G); virtually all type I fibers were affected. On NADH and SDH reactions, both patients showed fibers that contained core-like areas devoid of oxidative enzyme activity and several ring fibers (Figure 4H and I). On ATPase staining, there was type I fiber predominance and hypertrophy; most type II fibers were atrophic. Double labeling immunohistochemistry for slow and fast myosin isoforms revealed marked predominance and hypertrophy of type I (slow) fibers, and atrophy of type II (fast) fibers. A few atrophic fibers co-expressed both slow and fast myosin (Figure 4J). No immature fibers were observed. Rods and most of the core-like areas showed strong α-actinin, filamin C, and myotilin immunofluorescence (Figure 5). Faint overexpression of desmin was seen in the cytoplasm of several fibers. More enhanced desmin immunoreactivity was present under the sarcolemma, or diffusely within the cytoplasm of atrophic fibers. However, fiber areas corresponding to rods and core-like lesions displayed no desmin immunoreactivity (data not shown).

Electron-microscopic study uncovered numerous abnormal electron-dense structures corresponding to rods; they protruded from the Z-lines and ran in a perpendicular direction (Figure 6A and C). The sarcomere structure was preserved in some fibers (Figure 6C), but it was severely disorganized in others (Figure 6A,E,F). On transverse sections collections of small rods were observed (Figure 6D). The core-like areas seen on light microscopy corresponded to regions where rods were abundant and the myofibrillar disruption was the heaviest (Figure 6A,E,F). Some muscle fibers contained massive electrondense filamentous material, probably of Z-disk origin but few rod-like structures (Figure 6E and F). Clusters of mitochondria were seen at the periphery of the disorganized sarcomeres. The myopathological diagnosis of nemaline myopathy was established based on the presence of nemaline rods as the most relevant myopathologic feature (although additional core-like lesions were present) and the absence of findings indicative of other disorders in which nemaline bodies may also be present (for diagnostic criteria – see ref. 7).

Chromosomal assignment and candidate gene screening

Autosomal dominant inheritance is reliably confirmed in this Spanish family by the fact that the disease was inherited from a man in his two consecutive marriages and the evidence of male-to-male transmission (Figure 1). Screening of the coding exons of genes associated with autosomal dominant NEM, *ACTA1*, *TPM3*, and *TPM2* did not uncover meaningful changes. In addition, *CFL2* and *TNNT1* (but not *NEB*) genes implicated so far in autosomal recessive NEM, were also analyzed, and no mutations were found. Genotyping with microsatellite markers in the 15q21-q23 region that contains the putative unknown NEM6 gene [23] resulted in the identification of a disease-associated 3-3-2-1-6 haplotype shared by all affected but not the unaffected members of the family (Figure 1). The estimated LOD score for linkage to the 15q21-q23 locus is 2.077. Suggestive linkage and the perfect segregation of the disease-associated haplotype indicate that nemaline myopathy in this family is linked to the same 15q21-q23 chromosomal region as in the Dutch and Australian-Dutch families [23]. Eighteen genes located in the candidate region segregating with the disease, including *ANXA, TPM1, Talin 2, LACT, RABB, HERC1, DAPK2, UPB3, PARP16, PPIB, MEMT, RASL12, CLPX, C15orf44, NOPE, SCL24A1, RAB11A, and DIS3L* were screened, but the search failed to uncover a causative mutation. Genotyping in the *RYR1* locus on chromosome 19q12-q13.2 excluded *RYR1* gene involvement in this disease (not shown).

DISCUSSION

Affected members of this nemaline myopathy family show phenotypic similarity with the syndrome previously characterized in Dutch and Australian-Dutch families and should to be designated NEM6 [22,23]. Shared clinical features include symmetric slowly progressive proximal muscle weakness that starts around 4 or 5 years of age. These Spanish patients show in addition distal muscle involvement, a feature that has not been observed in the reported 15q-linked families, except for a single patient of the Australian-Dutch family who showed weakness of ankle dorsiflexors [23]. Most significantly, the affected members of the Spanish family demonstrate slowness of movements that was previously described as a characteristic feature of the 15q-linked nemaline myopathy families [23] “Slow walking” was also mentioned in members of a family with nemaline myopathy due to mutations in the TPM3 gene [24] and therefore is not unique to the 15q type of disease. Muscle imaging studies were performed in three affected individuals. In the oldest patients diffuse involvement of the thigh muscles was observed, similarly to what has been previously found in patients who suffer from nemaline myopathy due to ACTA1 mutations. This is clearly different from the selective involvement of the anterior compartment seen in patients who carry mutations in the NEB gene[25]. At the mid-leg level muscle changes were more pronounced in lateral and

medial gastrocnemius, peroneal group and soleus, with less prominent involvement of the anterior tibialis. This is in contrast with the predominant involvement of the anterior tibialis and soleus muscles in patients with nemaline myopathy caused by NEB mutations, and from the relative sparing of the gastrocnemius seen in patients who carry ACTA 1 mutations[25].

Analysis of muscle biopsies revealed striking similarities with phenomena described in the Dutch and Australian-Dutch 15q-linked families [22,23]. These consisted of frequent nemaline bodies, prominent myofibrillar disorganization resulting in core-like formations, type I fiber predominance and hypertrophy, and type II fiber atrophy. Decreased oxidative enzyme activity in areas containing abundant rods occurs in various subtypes of nemaline myopathy and therefore is not specific for NEM6 [26]. However, in addition to these pseudo-core lesions we also found foci of complete myofibrillar dissolution appearing as aggregates of irregular filamentous electron-dense material and having none or only a few small rod-like structures. Similar abnormalities have been observed in the previously reported NEM6 families [22,23]. The combination of nemaline rods and core-like lesions has also been found in some patients with nemaline myopathy due to ACTA1 gene mutations [27]. However, it is noteworthy that the pseudo-core and core-like lesions observed in NEM6 cases and some nemaline myopathy patients who carry ACTA 1 mutations [27] differ from the classical sharply demarcated cores observed in the central-core or core-rod disease associated with RYR1 [19,20] or NEB [21] mutations. Another unifying feature of the NEM6 variant is the predominance and hypertrophy of type I vs. atrophic type II fibers. An abnormal fiber type I/ type II ratio is a frequent feature in nemaline myopathies, but most commonly this would be type I fiber predominance and atrophy, not hypertrophy, [5,18,24], and only a minority of characterized cases [18] show the pattern characteristic of the NEM6 patients.

Additional findings in the patients reported here was the presence of eosinophilic material in some fibers, probably corresponding to areas of myofibrillary dissolution and massive rod accumulation. This type of inclusion, is therefore different from the hyaline bodies observed in myosin storage myopathy[27]. In addition to previous observations of α-actinin[13,14] and myotilin[15] expression in rods, this study revealed filamin C immunofluorescence in rods, thus expanding our knowledge regarding rod body composition.

Considering the phenotypic similarity to the previously reported NEM6 families, we performed genotyping of 11 family members in the 15q21-q23 region by using some of the same markers employed in the studies of the Dutch and Australian-Dutch families 23. The disease-associated 15q haplotype perfectly co-segregates with the disease, suggesting that nemaline myopathy in the Spanish family is allelic to the Dutch and Australian-Dutch families. If we assume that the same unknown mutant gene causes nemaline myopathy in the Spanish, Dutch and Australian-Dutch families, it must be located in a 7-megabase region between markers D15S155 and D15S125 on chromosome 15q22.31, based on a recombination previously identified in the Dutch and Australian-Dutch families [23]. This interval contains the fast α-tropomyosin (TPM1) gene that has not been implicated in nemaline myopathy so far, but TPM1 mutations have been known to cause familial hypertrophic cardiomyopathy type 3 [29] and dilated cardiomyopathy 30. Analysis of the TPM1 gene in the Dutch, Australian-Dutch and now Spanish patients has not identified any causative changes. Eighteen other genes with known or unknown function have been screened in patients in the Spanish family, but to-date no pathogenic mutations have been found. The Spanish family is the third family genetically linked to the NEM6 chromosomal region; further studies of these three families will help to identify the NEM6 gene.

Acknowledgments

The authors are grateful to the patients and the members of the affected families for the enthusiastic participation in the study. This work was supported in part by a FIS grant PI08-574 (MO), USUHS R080CD (NS), the Intramural Research Program of the National Institute of Neurological Disorders and Stroke, National Institutes of Health (LGG, HSL, ZO), and the Australian National Health and Medical Research Council, Principal Research Fellowship 403904 (NGL). We acknowledge the support of Dr. S. Muldoon and Biomedical Instrumentation Center of the Uniformed Services University of the Health Sciences, Bethesda, Maryland, U.S.A.

Abbreviations

ATP	adenosine triphosphatase
CK	creatine kinase
CT	computed tomography
ECG	electrocardiogram
EMG	electromyography
HE	haematoxylin and eosin
MR	magnetic resonance
MRC	Medical Research Council
NADH	nicotinamide adenine dinucleotide dehydrogenase
NEM	nemaline myopathy
PCR	polymerase chain reaction
SE	spin echo
SDH	succinic dehydrogenase
STIR	short-time inversion recovery

References

1. Shy GM, Engel WK, Somers JE, Wanko T. Nemaline myopathy. A new congenital myopathy. Brain 1963;86:793–810. [PubMed: 14090530]
2. Nienhuis AW, Coleman RF, Brown WJ, Munsat TL, Pearson CM. Nemaline myopathy. A histopathologic and histochemical study. Am J Clin Pathol 1967;48:1–13. [PubMed: 4165764]
3. Engel AG, Gomez MR. Nemaline (Z disk) myopathy: observations on the origin, structure, and solubility properties of the nemaline structures. J Neuropathol Exp Neurol 1967;26:601–619. [PubMed: 6053732]
4. Karpati G, Carpenter S, Andermann F. A new concept of childhood nemaline myopathy. Arch Neurol 1971;24:291–304. [PubMed: 4251331]
5. North KN, Laing NG, Wallgren-Pettersson C. Nemaline myopathy: current concepts. The ENMC International Consortium on Nemaline Myopathy. J Med Genet 1997;34:705–713. [PubMed: 9321754]
6. Sanoudou D, Beggs AH. Clinical and genetic heterogeneity in nemaline myopathy — a disease of skeletal muscle thin filaments. Trends Mol Med 2001;7:362–368. [PubMed: 11516997]
7. Wallgren-Pettersson C, Laing NG. Report of the 70th ENMC International Workshop: Nemaline myopathy, 11–13 June 1999, Naarden, The Netherlands. Neuromuscul Disord 2000;10:299–306. [PubMed: 10838258]
8. Laing NG, Wilton SD, Akkari PA, Dorosz S, Boundy K, Kneebone C, et al. A mutation in the alphatropomyosin gene TPM3 associated with autosomal dominant nemaline myopathy NEM1. Nat Genet 1995;9:75–79. [PubMed: 7704029]

9. Pelin K, Hilpelä P, Donner K, Sewry C, Akkari PA, Wilton SD, et al. Mutations in the nebulin gene associated with autosomal recessive nemaline myopathy. Proc Natl Acad Sci U S A 1999;96:2305–2310. [PubMed: 10051637]
10. Nowak KJ, Wattanasirichaigoon D, Goebel HH, Wilce M, Pelin K, Donner K, et al. Mutations in the skeletal muscle alpha actin gene in patients with actin myopathy and nemaline myopathy. Nat Genet 1999;23:208–212. [PubMed: 10508519]
11. North KN, Laing NG. Skeletal alpha-actin diseases. Adv Exp Med Biol 2008;642:15–27. [PubMed: 19181090]
12. Wallgren-Pettersson C, Rapola J, Donner M. Pathology of congenital nemaline myopathy: a follow-up study. J Neurol Sci 1988;83:243–257. [PubMed: 3356991]
13. Wallgren-Pettersson C, Kääriäinen H, Rapola J, Salmi T, Jääskeläinen J, Donner M, et al. Genetics of congenital nemaline myopathy: a study of 10 families. J Med Genet 1990;27:480–487. [PubMed: 2213842]
14. Wallgren-Pettersson C, Jasani B, Newman GR, Morris GE, Jones S, Singhrao S, et al. Alpha-actinin in nemaline bodies in congenital nemaline myopathy: immunological confirmation by light and electron microscopy. Neuromusc Disord 1995;5:93–104. [PubMed: 7767098]
15. Schröder R, Reimann J, Salmikangas P, Clemen CS, Hayashi YK, Nonaka I, et al. Beyond LGMD 1A: myotilin is a component of central core lesions and nemaline myopathy. Neuromuscul Disord 2003;13:451–55. [PubMed: 12899871]
16. Gurgel-Giannetti J, Reed U, Bang ML, Pelin K, Donner K, Marie SK, et al. Nebulin expression in patients with nemaline myopathy. Neuromusc Disord 2001;11:154–162. [PubMed: 11257471]
17. Ryan MM, Ilkovski B, Strickland CD, Schnell C, Sanoudou D, Midgett C, et al. Clinical course correlates poorly with muscle pathology in nemaline myopathy. Neurology 2003;60:665–673. [PubMed: 12601110]
18. Agrawal PB, Greenleaf RS, Tomczak KK, Lehtokari VL, Wallgren-Pettersson C, Wallefeld W, et al. Nemaline myopathy with minicores caused by mutation of the CFL2 gene encoding the skeletal muscle actin-binding protein cofilin-2. Am J Hum Genet 2007;80:162–167. [PubMed: 17160903]
19. Monnier N, Romero NB, Lerale J, Nivoche Y, Qi D, Mac Lennan DH, et al. An autosomal dominant congenital myopathy with cores and rods is associated with a neomutation in the RYR1 gene encoding the skeletal muscle ryanodine receptor. Hum Mol Genet 2000;9:2599–2608. [PubMed: 11063719]
20. Scacheri PC, Hoffman EP, Fratkin JD, Semino-Mora C, Senchak A, Davis MR, et al. A novel ryanodine receptor gene mutation causing both cores and rods in congenital myopathy. Neurology 2000;55:1689–1696. [PubMed: 11113224]
21. Romero NB, Lehtokari VL, Quijano-Roy S, Monnier N, Claeys KG, Carlier RY, et al. Core-rod myopathy caused by mutations in the nebulin gene. Neurology 2009;73:1159–1161. [PubMed: 19805734]
22. Gommans IM, van Engelen BG, ter Laak HJ, Brunner HG, Kremer H, Lammens M, et al. A new phenotype of autosomal dominant nemaline myopathy. Neuromuscul Disord 2002;12:13–18. [PubMed: 11731279]
23. Gommans IM, Davis M, Saar K, Lammens M, Mastaglia F, Lamont P, et al. A locus on chromosome 15q for a dominantly inherited nemaline myopathy with core-like lesions. Brain 2003;126:1545–1551. [PubMed: 12805120]
24. Clarke NF, Kolski H, Dye DE, Lim E, Smith RL, Patel R, et al. Mutations in TPM3 are a common cause of congenital fiber type disproportion. Ann Neurol 2008;63:329–337. [PubMed: 18300303]
25. Jungbluth H, Sewry CA, Counsell S, Allsop J, Chattopadhyay A, Mercuri E, et al. Magnetic resonance imaging of muscle in nemaline myopathy. Neuromuscul Disord 2004;14:779–784. [PubMed: 15564032]
26. Dubowitz, V.; Sewry, CA. Muscle biopsy: A practical approach. 3. Saunders Elsevier; London: 2007. Congenital myopathies; p. 407-442.
27. Jungbluth H, Sewry CA, Brown SC, Nowak KJ, Laing NG, Wallgren-Pettersson C, et al. Mild phenotype of nemaline myopathy with sleep hypoventilation due to a mutation in the skeletal muscle alpha-actinin (ACTA1) gene. Neuromuscul Disord 2001;11:35–40. [PubMed: 11166164]

28. Oldfors A. Hereditary myosin myopathies. Neuromuscul Disord 2007;17:355–367. [PubMed: 17434305]

29. Thierfelder L, Watkins H, MacRae C, Lamas R, McKenna W, Vosberg HP, et al. Alpha-tropomyosin and cardiac troponin T mutations cause familial hypertrophic cardiomyopathy: a disease of the sarcomere. Cell 1994;77:701–712. [PubMed: 8205619]

30. Olson TM, Kishimoto NY, Whitby FG, Michels VV. Mutations that alter the surface charge of alpha-tropomyosin are associated with dilated cardiomyopathy. J Molec Cell Cardiol 2001;33:723–732. [PubMed: 11273725]

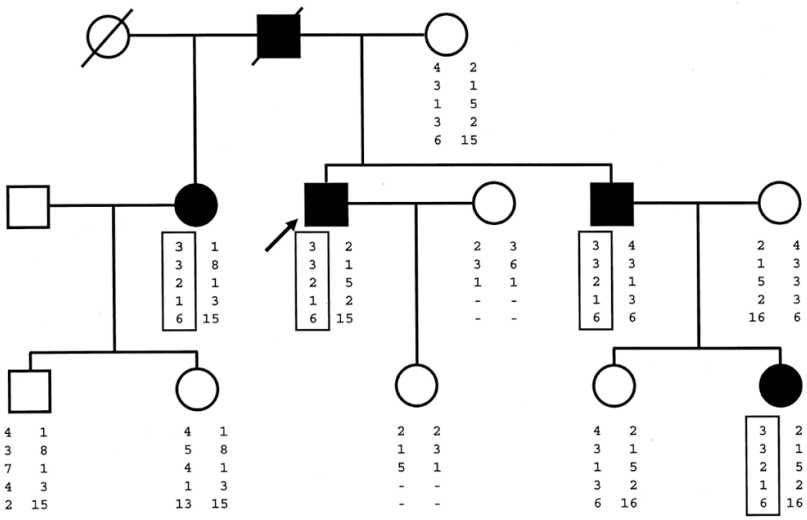

Figure 1.

Pedigree of the Spanish nemaline myopathy family. Filled symbols indicate individuals affected with myopathy; empty symbols represent unaffected family members. Bracketed bars indicate disease-associated haplotype constructed with the use of chromosome 15q marker alleles. The marker order, from centromere to telomere, is D15S1033, D15S1036, D15S1507, D15S153. D15S131.

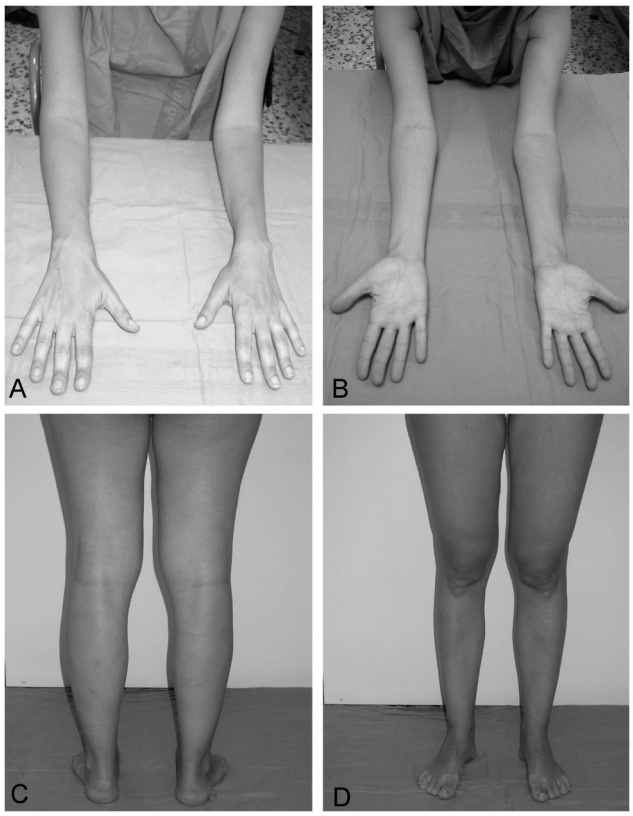

Figure 2.
Upper limb hypotrophy (**A** and **B**), particularly of forearm muscles, in contrast with relatively preserved muscle bulk in lower limbs (**C** and **D**) in individual III:5.

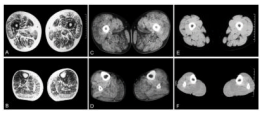

Figure 3.
Magnetic resonance imaging of the lower extremities of patient II:3 showing diffuse fatty replacement of thigh (**A**) and leg muscles (**B**), specially in the lateral and medial gastrocnemius, peroneal group and soleus, with less prominent involvement of the anterior tibialis. The same pattern of muscle involvement was observed on muscle CT scans in patient II:5 (**C**, **D**). In the younger individual (III:5), minor abnormalities were observed (**E**, **F**).

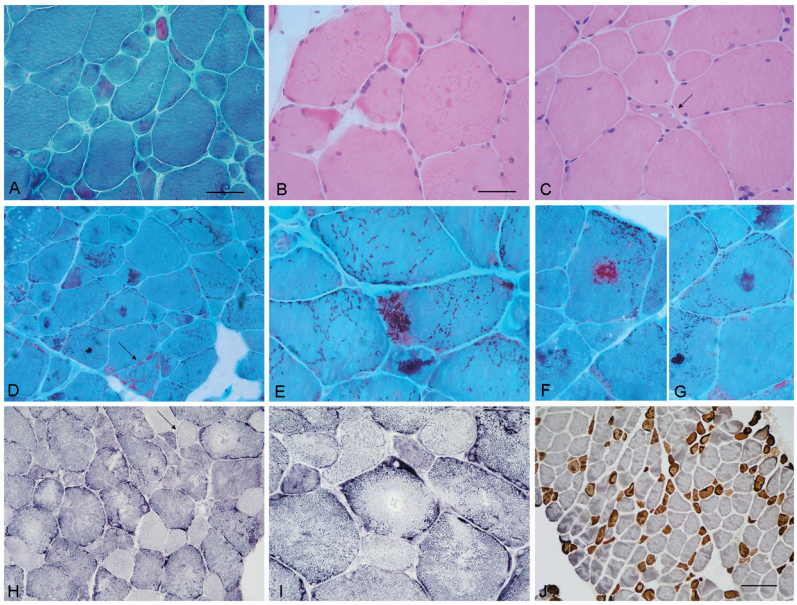

Figure 4.

Histochemical findings in individuals II:3 (**A** to **C**), and II:5 (**D** to **J**) of the Spanish nemaline myopathy family. (**A**) Marked variation in the fiber size; abnormal multiple small or confluent dark-green to red-purple inclusions in the cytoplasm. (**B**) Areas corresponding to rods appear eosinophilic on H&E stain; some fibers contain hyaline material in areas under the sarcolemma. (**C**) Rimmed vacuoles in an atrophic fiber (arrow). (**D**) Marked variation in the fiber size and mildly increased connective tissue. Aggregates of typical nemaline rods in multiple fibers; isolated ragged red fibers (arrow). (**E**) Clusters of rods in areas under the sarcolemma and centrally within the cytoplasm. (**F** and **G**) In addition to smaller rods, some fibers contain confluent red or purple inclusions. (**H** and **I**) Oxidative stain reaction showing multiple core-like areas and ring fibers (arrow). (**J**) Double labeling immunohistochemistry for slow (grey) and fast (brown) myosin demonstrating type I fiber predominance and hypertrophy and type II fiber atrophy. Bar in **A** (**A**, **D** and **H**) = 100 μm; Bar in **B** (**B**, **C**, **E**, **F**, **G** and **I**) = 50μm; Bar in **J** = 200 μm.

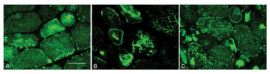

Figure 5.
Immunocytochemical analysis with fluorescein-conjugated monoclonal antibodies in muscle biopsy from individual II: 5, showing prominent α-actinin (**A**), filamin C (**B**), and myotilin (**C**) expression in rods and in some core-like areas. A ring fiber is visible in **C** (arrow). Bar in **A** (**A** to **C**) = 50 μm.

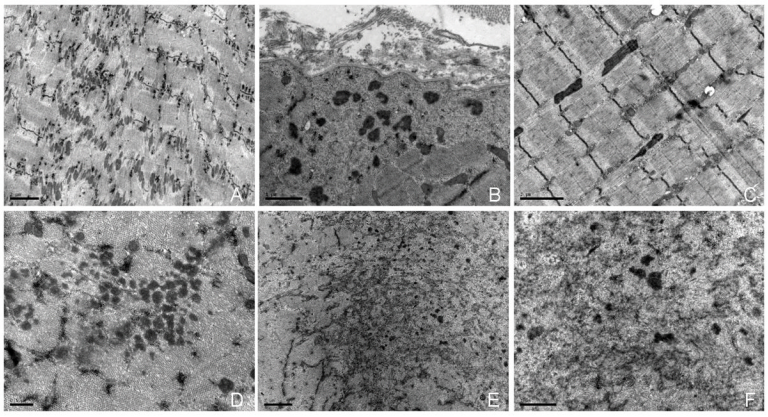

Figure 6.

Ultrastructural findings in patients II:3 and II:5 of the family. (**A**) Nemaline rods emanating from the Z-disks and resulting in sarcomere disorganization in heavily affected cells. (**B**) Aggregates of rod bodies located under the sarcolema or (**C** and **D**) between the myofibrils. (**C**) Typical rods in a fiber with well preserved sarcomere structure. (**E**) Complete dissolution of the myofibrils in a region occupied by electron dense filamentous material, and (**F**) on higher magnification, destructive filamentous masses probably of Z-disk origin containing only a few rod-like bodies.